Clin. Lab. 2015;61:XXX-XXX

ORIGINAL ARTICLE

Expression Analysis of p16, c-Myc, and mSin3A in Non-small Cell Lung Cancer by Computer Aided Scoring and Analysis (CASA)

Arash Salmaninejad [1], Mehrdad Asghari Estiar [1], Rajbir K. Gill [2], Joanna H. Shih [3], Stephen Hewitt [4], Hyo-Sung Jeon [5], Junya Fukuoka [6], Konstantin Shilo [7], Abbas Shakoori [1, 2, 3], Jin Jen [8]

[1] *Department of Medical Genetics, Cancer Institute of Iran, Tehran University of Medical Sciences, Tehran, Iran*
[2] *Laboratory of Human Carcinogenesis, Center for Cancer Research, National Cancer Institute, Bethesda, MD, USA*
[3] *National Cancer Institute, Executive Boulevard, Bethesda, Maryland, USA*
[4] *Center for Cancer Research, National Cancer Institute, National Institutes of Health, Bethesda, MD, USA*
[5] *Department of Biochemistry and Cell Biology, School of Medicine, Kyungpook National University, Daegu, South Korea*
[6] *Department of Pathology, Nagasaki University Graduate School of Biomedical Sciences, Sakamoto, Nagasaki, Japan*
[7] *Department of Pulmonary & Mediastinal Pathology, Armed Forces Institute of Pathology, Washington, DC, USA*
[8] *Department of Laboratory Medicine and Pathology, Mayo Clinic, Rochester, MN, USA*

SUMMARY

Background: **Immunohistochemical analysis (IHC) of tissue microarray (TMA) slides enables large sets of tissue samples to be analyzed simultaneously on a single slide. However, manual evaluation of small cores on a TMA slide is time consuming and error prone.**

Methods: **We describe a computer aided scoring and analysis (CASA) method to allow facile and reliable scoring of IHC staining using TMA containing 300 non-small cell lung cancer (NSCLC) cases. In the two previous published papers utilizing our TMA slides of lung cancer we examined 18 proteins involved in the chromatin machinery. We developed our study using more proteins of the chromatin complex and several transcription factors that facilitate the chromatin machinery. Then, a total of 78 antibodies were evaluated by CASA to derive a normalized intensity value that correlated with the overall staining status of the targeting protein. The intensity values for TMA cores were then examined for association to clinical variables and predictive significance individually and with other factors.**

Results: **Using our TMA, the intensity of several protein pairs were significantly correlated with an increased risk of death in NSCLC. These included c-Myc with p16, mSin3A with p16 and c-Myc with mSinA. Predictive values of these pairs remained significant when evaluated based on standard IHC scores.**

Conclusions: **Our results demonstrate the usefulness of CASA as a valuable tool for systematic assessment of TMA slides to identify potential predictive biomarkers using a large set of primary human tissues.**

(Clin. Lab. 2015;61:xx-xx. DOI: 10.7754/Clin.Lab.2014.141125)

Correspondence:
Abbas Shakoori, MD, PhD
Department of Medical Genetics
Cancer Institute of Iran
Tehran University of Medical Sciences
Keshavarz Blvd
Tehran 13145-158, Iran
Phone: +9821 66914545
Email: shakooria@tums.ac.ir

Jin Jen, MD, PhD
Department of Laboratory Medicine and Pathology
Mayo Clinic
Rochester, MN, USA
Phone: +1 507-284-0526
Email: Jen.Jin@mayo.edu

Manuscript accepted November 24, 2014

KEY WORDS

tissue microarray, immunohistochemistry, Computer Aided Scoring and Analysis (CASA), NSCLC

INTRODUCTION

Lung cancer is one of the major cancers throughout the world with high frequency, mortality and little effective therapy [1]. Lung cancer develops through a multistage procedure involving a variety of genetic and epigenetic alterations in different genes [2]. NSCLC accounts for approximately 85% of all lung cancer subtypes and can be further categorized into adenocarcinoma (39%), squamous cell carcinoma (21%), large cell carcinoma adenocarcinoma (3%), and uncommon types and combined types encompassing the remaining 22% [3]. Novel approaches for screening and treatment have begun to make a momentous influence on the burden of this disease and advances in lung cancer screening using low-dose computed tomography (CT) scans and tissue microarray (TMA) have confirmed to be profitable [4]. Although intensive research has been conducted, understanding and management of NSCLC is only slightly improved. Meanwhile, comprehensive histopathological features and identified clinical prognostic factors limited the prediction of lung cancer outcome.

The TMA is a form of large scale parallel histopathology where several hundred tissue specimens are placed onto a single slide for simultaneous analysis. This technology commonly uses formalin fixed parafin embedded (FFPE) tissue or acetone-fixed frozen tissue [5]. The development of TMA allows for simultaneous examination of a large number of samples on the array and is amenable for protein, RNA, as well as DNA analysis [6-9]. Gene expression profiles by cDNA microarray studies have brought new insights into molecular mechanisms of diseases [10,11]. However, large scale RNA analysis on tissues often requires fresh frozen specimens, limiting its application for routine clinical use. In order for a molecular marker to be readily usable in the clinical settings, assessment of the candidate gene in FFPE tissues is desired since they are readily available and are the primary media of tissue preservation in diagnostic pathology. Indeed, TMA is increasingly used in molecular epidemiology, drug development, and in determining the diagnostic, prognostic and predictive value of new tissue biomarkers [12,13]. It has also been used as a proteomic tool for both basic and clinical investigation [14].

Recently, automated instrumentations and analytical tools have been developed to aid the archiving and interpretation of data through digital image analysis. Technology exists to obtain and store digital images of stained tissue samples. However, the evaluation of the antigen expression patterns is mostly conducted manually [15-18]. Automated analysis is a potentially beneficial tool for complex analysis such as identification of correlations between multiple protein expressions within a signaling pathway and profiling of the human proteome. It also allows dealing with organizing genetic information such as structurally correlated single nucleotide polymorphisms (SNPs) [19,20]. Many of these systems have demonstrated efficiency in TMA image analysis [21]. However, algorithm modifications, sample core variations, and normalizations among different experiments remain critical factors that limited its utility for systematic analysis of TMA images. There are numerous semi automated methods (ACIS, AQUA) to evaluate expression of proteins on TMA slides but they utilize double TMA slides one for targeted protein and another for cytocreatins as housekeeping proteins as a control for normalizing of computer scores [22-24]. Here we describe a CASA method which allows IHC staining to be systematically scored. The CASA method utilizes available digital imaging systems to obtain IHC staining information and then systematically normalizes the images to allow accurate representation of the protein status in the entire cell. This high-throughput method allows for rapid and robust analysis of protein expression and association in clinical samples. To test this approach, we applied CASA analysis using a lung cancer TMA containing 150 adenocarcinoma (AD) and 150 squamous cell carcinoma (SCC) cases [25,26].

Using manual scoring in our previous published papers, we examined 18 proteins involved in the chromatin machinery [25,26]. In this paper, a total number of 78 antibodies, mostly known to be associated with cancer development as well as a set of chromatin remodeling proteins, were subjected to CASA analysis [27]. Association of CASA scores together with related clinical data were analyzed among all antibodies with optimal staining.

MATERIALS AND METHODS

Clinical samples and NSCLC TMA

Three hundred lung cancer cases (150 pulmonary AD and 150 SCC cases) were selected from the Armed Forces Institute of Pathology archive, based on the diagnosis and the quality and quantity of the available tissue on the paraffin block under the approved IRB from associated institutions. Cylindrical tissue cores with the diameter 0.6 mm were selected from the original donor blocks and were extruded directly into the recipient block with coordinated wells. The details for construction of the TMA was previously described [25,26]. Demographic and clinical data were collected at the time of block acquisition or through the National Death Registry record (Table 1). A total of 267 patients had complete clinical information. Survival time and outcome data were available for 254 patients. The tumors were staged according to the International Union against Cancer's tumor node-metastasis (TNM) classification and were subtyped and graded according to the WHO guidelines as previously described [25,26].

Antibody selection, immunohistochemical staining, and manual scoring

The primary selection of the antibodies was based on the knowledge of the protein participation in cancer development or chromatin remodeling machinery, [25] and the transcription factors which facilitated by chromatin modifying and remodeling machinery [27]. Then we considered the commercial availability of the antibodies and reliability of the immunohistochemical staining. A total of 78 antibodies involving 112 TMA slides which were used for IHC staining on the TMA slides were included in the association analysis based on the quality of the TMA and the IHC staining (Figure 1) (Supplementary Table 1). Many of the antibodies were known or suggested to be a diagnostic or prognostic marker of cancer, especially in lung cancer [28-33]. Recently, we maintained the unique method for IHC that enables us to improve the reliability of digital analysis. We used the same secondary antibodies as well as visualization reagents (EnVision®+ DAB kit, DakoCytomation, Carpinteria, CA). The detailed protocol for IHC and manual scoring has been previously described [25,26].

A pathologist (JF) manually scored all IHC staining in the TMA prior to CASA analysis. The criteria for the staining were manually scored as follows: distribution score was scored as 0 (0%), 1 (1 - 50%), and 2 (51 - 100%) to indicate the percentage of positive cells in all tumor cells present in one tissue. The intensity of the signal (intensity score) was scored as 0 (no signal), 1 (weak), 2 (moderate), and 3 (marked). The total of distribution score and intensity score was then summed into a total score (TS) of TS0 (sum 0), TS1 (sum 2), TS2 (sum 3), and TS3 (sum 4 - 5). Throughout this study, TS0 or TS1 was regarded as negative, whereas TS2 or TS3 was regarded as positive.

For manual scoring, tissue cores with questionable signals due to insufficient tumor cells, which were difficult to distinguish from other inflammatory or interstitial cells or tissues with homogenously weak signals, were excluded from further evaluation. Cores with only necrotic tumor cells or tissues with highly homogenous background were also excluded. Twenty-seven cases with an intensity score of 3 by all manually tested antibodies were excluded from all analysis. Furthermore, due to the small size of tissue samples in TMA, approximately 10% of the positive samples could be scored as negative due to sampling [25,26]. Interpretation of immunohistochemistry staining data was based on recognition of signal deposits, brown in most cases, among specific cells and tissue structures. The general parameters of these analyses include intensity, localization, and proportion of cells of interest that showed specific staining. This interpretation is typically qualitative in nature using negative/positive or 0, 1, 2, 3 scoring systems. The manual scores for some of the proteins were published previously [25,26].

Optimization and normalization of pixel intensity values

IHC stained TMA slides were scanned by the Aperio ScanScope® GL System and reviewed by Aperio ImageScope software (version 7.3.36). The slide images were transferred to Aperio-TMA lab image analysis software (version 7.0.1.235), dearrayed back to individual cores and analyzed using the Aperio's Pixel Count Algorithm in the TMALab image software. The algorithm obtains a pixel intensity value of DAB dye (brown color) regardless of subcellular localization (Figure 2). To improve the protein staining signals, pixels within the minimum pixel intensity (scale 1 - 50) were excluded from the algorithm because they represented the nonspecific anthracotic dust deposit or DAB accumulated particles. Then the maximum pixel range (scale 190 - 220) were excluded from the algorithm because they represented HRP/DAB deposition particles on TMA slides or stromal cells staining which were near to background. Thus, the final specific brown stains representing the targeting protein in the sample were calculated as a sum of all pixels with the intensity between 50 - 190.

The normalization steps included: I) exclusion of missing cores or cores that were too small to be analyzed (pixel count < 200,000 or approximately < 20% max pixel, involving ~10% cores/slide), II) size normalization to adjust for size variations among the core samples. We normalized based on the average pixel count of the full core (1,000,000 pixels) using the formula: size normalized score = intensity of brown color x (1,000,000 pixels/number of pixels in the core), and III) intensity normalization to adjust for staining intensity differences among the experiments and slides. The average of 78 IHC stains had a maximum value of 120,000,000. Thus all cores are adjusted based on ratio to 120,000,000 using the formula: intensity normalized score = size normalized score x (120,000,000/maximum value in the slide).

Statistical analysis

To evaluate the overall performance of CASA scores, receiver operating characteristic curve analysis (R.O.C Analysis software, Department of Radiology, Johns Hopkins University) was performed. The 0, 1, 2, and 3 routine pathology scores were converted to negative (0 or 1) or positive (2 and 3) for survival analysis. The manual scores (negative/positive) of 19 proteins that had been previously analyzed [25,26] were compared with CASA scores using the ROC method. In addition, eight duplicated TMA slides were stained using the same antibody and method to determine the overall correlation coefficient among different array slides. The association of each protein with common clinical variables was explored using two-tailed *t*-test and assuming equal variance after log transfer of CASA scores. $P < 0.01$ was considered significant. Association of clinicopathological factors such as age, gender, stage, and

histology type were considered statistically significant if $p < 0.01$ for the two-tailed *t*-test.

Cox Proportional-hazards survival regression was performed individually for each marker using log-transformed CASA scores by Epi Info (version 3.3.2). Wald's p-values were considered significant in protein markers and in clinical variables: age, gender, stage, and histology were significant if $p < 0.01$. Stepwise Cox Proportional-hazards survival regression was performed by SAS (version 8.02) in a forward model. Pathway classifications of 78 antibodies were obtained based on Ingenuity Pathway Analysis (IPA). Proteins of the same cluster and clinical factors (age, gender, tumor stage, histology) were entered together for multivariate analysis and then followed by forward stepwise analysis until the highest significant likelihood ratio was reached. Pair-wise Cox Proportional-hazards survival regression was performed among the set of proteins identified by forward stepwise analysis. A likelihood ratio test was used to calculate p-values; those less than 0.01 were considered significant. Log-transformed CASA scores for each group of IPA antibodies were subjected to multivariate COX regression analysis and only proteins with a Wald's p-value < 0.01 were further compared with other proteins within the same cluster. Kaplan-Meier curves were used to estimate survival probability of paired proteins obtained from COX analysis using manual scores. The Wilcoxon test was considered significant if $p < 0.05$. Manual scores of 0 and 1 were regarded as low expression and manual scores of 2 and 3 as high expression.

Cluster analysis

A list of 78 gene symbols were subjected to Ingenuity pathway analysis (IPA) to assess the biological and functional relationships of the proteins in this study (Ingenuity IPA, Application Version: 6.3, Content Version: 1402).

For correlation analyses, hierarchical clustering (version 1.60) was used. Log transformed CASA scores of 78 antibodies were clustered using complete linkage clustering after 90% filtering and median center normalization. Finally, 55 TMA slides manually scored by J.F. were subjected to hierarchical cluster analysis.

RESULTS

Acquisition of CASA scores from immmunostained lung tissue microarray

We used the Aperio imaging algorithm to digitally acquire immunostaining images for each of the tissue cores present in a tissue microarray containing 300 NSCLC tumors. The algorithm of image software was modified before reading the image values. This type of software adjusts to count the image pixels from one to a scale based on the intensity of the color of the DAB-complex. We found that the only pixels within the middle part of the scale will represent the specific staining of protein. Thus, pixels within the maximum pixel intensity (scale 1 to 50) were excluded from the algorithm because they represented the nonspecific anthracotic dust deposit or DAB accumulated particles. Then the minimum pixel range (scale 190 to 220) was excluded from the algorithm because it represented HRP/DAB deposition particles on TMA slides or stromal cell staining which were near to background (Figure 2). The modified pixel intensity value for each core was then normalized to adjust for a core size at 1,000,000 pixels/core. Because of the variation in intensity among the slides varied greatly (72,000,000 - 172,000,000 pixels/slide), we normalized the maximum pixel count to the average of 120,000,000 pixels/slide for all slides to minimize variations in staining intensity among experiments. Furthermore, tissue core images with a pixel count < 200,000 were removed from digital scoring because they lacked sufficient tissue for scoring. This filtering retained 90% of the cores for further analysis compared to ~85% retention for manually scored slides (Figure 3a and 3b).

Reproducibility and reliability of CASA

The robustness of the CASA approach was evaluated using ROC curve analysis by comparing the CASA score from 19 proteins to the manual scores of the same IHC stained slide as generated by a trained pathologist. A maximum CASA score of 120,000,000 for a tissue core is equivalent to a manual pathology score of "3". However, we could not determine a cutoff in the continuous CASA scores from one to 120,000,000 to dichotomize CASA scores into two groups (negative and positive) or into four groups to show how they were equivalent to 0, 1, 2, and 3 manual scores (Figure 3a and 3b). The results of ROC curve analysis showed that the classification of samples using the CASA method had a similar degree of accuracy as compared to those scored manually (manual method is being used as the gold standard) (Figure 3c). The areas under the receiver operator curves of p16 and c-Myc proteins for manual scoring were 0.922 and 0.899, respectively. Similar analysis for 19 additional proteins showed 80% to 90% concordance (Figure 3c).

The clinical association of 55 manually scored TMA slides as well as hierarchical clustering was compared to the same slides of CASA scores. The results showed nearly identical results to those obtained using manual scorings versus CASA, demonstrating that computer-aided scoring analysis was comparable to manually scoring.

Because each TMA slide represents a distinct tissue area in the analysis, we also examined the reproducibility of CASA analysis by comparing the intensity scores on 10 slides with four different antibodies. We tested the variability of core to core using 3 or 2 TMA slides. This was performed by unique runs of the same tissues of lung cancer patients on different slides. Three TMA slides each were tested for XPC and PGP9.5 and two slides each were tested for TGFBR1 and FOXM1.

FOXM1 a and b, XPC a, b, and c slides were tested from the same TMA paraffin block but TGFBR1 a and b, PGP9.5 a, b, and c slides were from different TMA paraffin blocks. Under the same staining conditions the correlation coefficient of each duplicated experiments ranged from 64% for FOXM1 to 99% for XPC suggesting that the digital value generated by CASA is reproducible (data not shown).

Association of CASA scores with clinical variables

The primary objective of our work was to systematically examine whether biological molecules can be identified as a diagnostic or prognostic marker for cancer. Among 78 tested antibodies we found that LY-GDI was the only protein with a preference for patients greater than 60 years old ($p = 0.0048$). This is consistent with a previous report [34]. The expression of a few proteins (p16 and Her2) showed marginally significant association with age and gender ($p < 0.05$) (Supplementary Table 2). High expression of p14 and RB among our antibodies appeared to be significantly associated with the early stage (stage I and II, $p < 0.01$) (Supplementary Table 2). This is in line with several reports that document p14 and RB as tumor suppressor genes in lung cancer [35-37].

The CASA scores for 29 proteins showed significant association with histology subtype ($p < 0.01$). Of those, 20 proteins, the proteins such as TGFBR2, GSK3B and HER-2, were expressed significantly higher in adenocarcinomas while 9 proteins were expressed significantly higher in squamous cell carcinoma (Supplementary Table 2). The p63 gene, which is located in a region frequently amplified in squamous cell lung cancer, was one of the most significant factors in these tumors based on CASA scores. In addition, markers commonly known to be associated with particular NSCLC subtypes, thyroid transcription factor-1 (clone SPT24) and high molecular weight keratin (clone 34BE12), also had the most significant association to adenocarcinoma and squamous cell carcinoma, respectively (Supplementary Table 2). Similarly, HDAC2 and P-cadherin have not been known to be associated to squamous cells of lung cancer.

Hierarchical and ingenuity clustering in manual and computer aided scoring

We also subjected the CASA scores for all antibodies to hierarchical cluster analysis and ingenuity cluster analysis. A hierarchical cluster of 55 manually scored proteins was identical to the CASA scored protein. Comparison was performed between 78 proteins of hierarchical versus ingenuity cluster and the results showed the identity of both methods. For example, the Smad family of proteins and Desmoglein family of proteins were clustered together. However, we chose Ingenuity cluster data for statistical analysis because it more closely reflects a biological association rather than correlated expression. After log transformation, CASA values for all 78 antibodies were entered into IGA and subjected to classification based on the known molecular pathway associated with the tested proteins (Supplementary Figure 1).

Utilization of CASA to identify proteins that are associated with clinical outcome

We also tested whether CASA values could be used to identify candidate markers through association with patient survival. Among 300 samples subjected to TMA, 254 patients had complete clinical follow up (Table 1). Survival analysis was performed by Cox proportional-hazards model using log-transformed CASA scores. A total of 78 antibodies were entered with clinical characteristics such as gender, age, tumor stage, and histology (Table 2). Tumor stage was associated with a hazard risk of 1.33 ($p < 0.0008$) reflecting the association of advanced stage and reduced survival in NSCLC patients and is consistent with our Kaplan-Meier data reported previously [25,26]. In addition, male patients had marginally significant reduced survival compared to females ($p = 0.018$, HR 1.54). When considered individually, most antibodies did not have statistically significant prognostic values (Table 2).

We next performed stepwise analysis and multiple regression analyses based on the biological pathways identified by IPA analysis. Proteins in each of the five IPA groups were evaluated jointly or in pairs in the presence of commonly considered clinical factors using the Cox regression model. Of the IPA Cluster II consisting of 23 proteins, seven (p16, GGH, c-Myc, mSin3A, BAF155, BAF170, Talin) were jointly predictive for survival when considered together with tumor stage and gender.

To further identify the most informative factors, we evaluated their significance in pairs for overall patient survival (Table 3). The combination of c-Myc with p16, mSin3A with p16, c-Myc with mSin3A, and Her2 with Maspin showed significant association to survival ($p < 0.01$). Hazard ratios of these combinations showed that high c-Myc with low p16, high mSin3A with low p16, high c-Myc with high mSin3A, and high Her2 with low Maspin each had significant association to reduced survival (Table 3). The predictive significance remained strong when only Stage I patients were considered.

Correlation of pair-wise Cox analysis using CASA with patient survival using manual IHC scores to test the reliability of clinical outcomes obtained from CASA

Although highly informative, we recognize that CASA scores cannot be easily applied to clinical settings at this point, because of the need for another device to dichotomize continuous CASA scores. We therefore performed the Kaplan-Meier survival analysis of the predictive proteins identified through Cox analysis using IHC scores of the same TMA slides assessed by a pathologist. Consistent with Cox analysis, combinations of low p16 with high c-Myc and low p16 with high mSin3A were associated with worse overall survival in all pa-

Table 1. Clinical Characteristics of NSCLC patients.

Variable	Category	No. of patients * (%)	Median survival (years)
Gender	Female	72 (27%)	4.7
	Male	196 (73%)	3.9
Age (mean = 64 ± 9)	< 60	78 (29%)	4.3
	> 60	189 (71%)	4.0
Stage	I	142 (64%)	4.5
	II	38 (17%)	4.3
	III	33 (15%)	3.2
	IV	10 (4%)	2.6
Histology	Adenocarcinoma	150 (50%)	3.8
	Squamous cell carcinoma	150 (50%)	4.5
Alive		63 (25%)	7.0
Dead	Tumor related	49 (19%)	2.4
	Other cause	20 (8%)	3.6
	Unknown	123 (48%)	3.4
Follow up	Median	254	4.1

*** Indicate the number of available patients in each category.**

Table 2. Cox proportional-hazards model of individual variables.

Individual variables	Hazard ratio	95% C.I.	Coefficient	S. E.	Z-Statistic	Wald's p-value
Gender	1.5338	1.0765 - 2.1853	0.4277	0.1806	2.3679	0.0179
Age	1.0111	0.9948 - 1.0277	0.0111	0.0083	1.3328	0.1826
Histology	0.9152	0.6862- 1.2206	-0.0886	0.1469	-0.6032	0.5464
Stage	1.3325	1.1264 - 1.5763	0.287	0.0857	3.3478	0.0008
p16	0.6741	0.4956 - 0.9168	-0.3944	0.1569	-2.5132	0.012
Her2	1.6902	1.1148 - 2.5626	0.5248	0.2123	2.4716	0.0134
mSin3A	2.1995	1.0138 - 4.7719	0.7882	0.3952	1.9947	0.0461
Cyclin B1	2.9093	0.9943 - 8.5125	1.0679	0.5478	1.9495	0.0512
BCL2	0.6086	0.3672 - 1.0086	-0.4966	0.2577	-1.9268	0.054
c-Myc	1.5973	0.9919 - 2.572	0.4683	0.2431	1.9266	0.054

Cox proportional-hazards using four clinical factors and 6 proteins with lowest Wald's p-values. The proteins were listed by increasing p-values from p16 to c-Myc.

Table 3. Summary of pair-wise COX multivariate regression.

Protein name	All patients			Stage I patients		
	Hazard ratio	95% C.I.	Likelihood p-value	Hazard ratio	95% C.I.	Likelihood p-value
c-Myc p16	1.43	0.88 - 2.33	< 0.01	1.95	0.99 - 3.80	< 0.01
	0.66	0.48 - 0.90		0.49	0.31 - 0.79	
mSin3A p16	2.15	1.03 - 4.47	< 0.01	2.11	0.66 - 6.70	< 0.01
	0.63	0.46 - 0.69		0.53	0.3 - 0.84	
c-Myc mSin3A	1.69	1.04 - 2.76	< 0.01	2.29	1.12 - 4.70	0.0206
	2.24	1.08 - 4.65		2.16	0.69 - 6.80	
Her2 Maspin	2.10	1.35 - 3.26	< 0.01	2.50	1.26 - 4.96	< 0.01
	0.47	0.17 - 1.34		0.15	0.03 - 0.75	

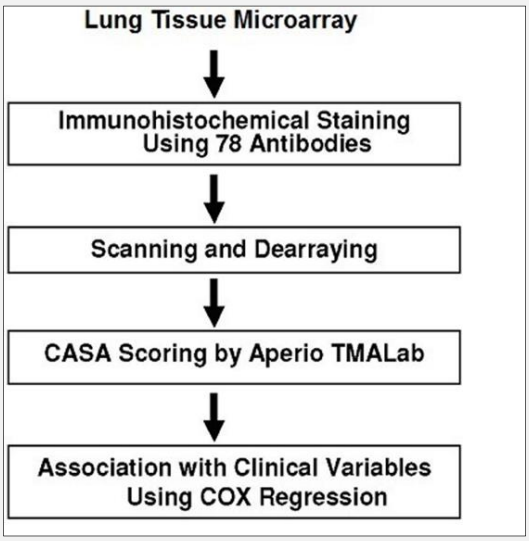

Figure 1. The schematic outline of computer aided scoring and analysis (CASA) using lung cancer TMA.

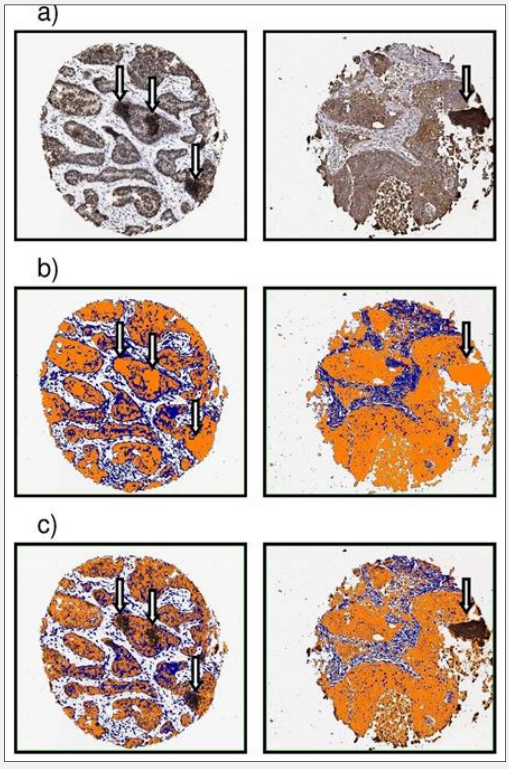

Figure 2. Example of two representative cores with black artifacts measured by positive pixel count algorithm.

a) The IHC staining of original images, brown color - IHC staining of target protein, blue color - hematoxilin staining, b) Original algorithm, orange color - area counted for pixel intensity values 1 - 220, c) The modified algorithm using pixel intensity values 50 - 190. Note the nonspecific black areas were excluded from pixel counting.

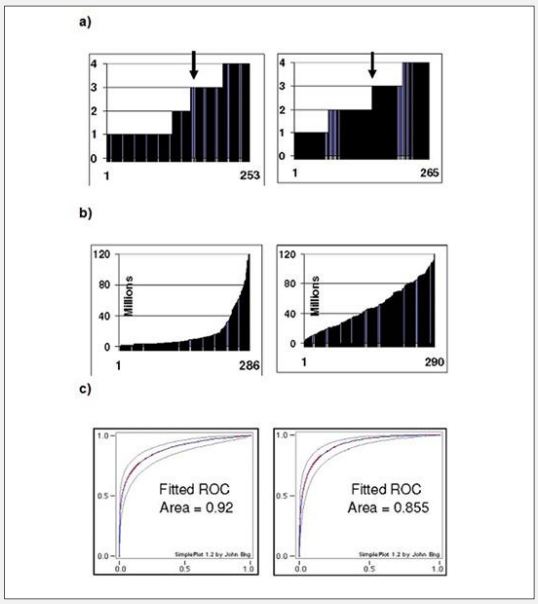

Figure 3. Comparison of manual and CASA scores.

Manual and CASA scores were compared in p16 (left panel) and c-Myc (right panel). Patients are sorted based on increasing of manual (a) or CASA scores (b) on X-axis. The CASA scores of 120,000,000 is equivalent to pathology score of "4" in manual scores. Arrows indicate negative and positive cutoff using manual scores. c) R.O.C curve of each pair of manual scores and CASA score in same score. The fitted R.O.C areas are as shown. R.O.C. curve analysis demonstrated the concordance of the two methods at 92% for p16 and 85% for cMyc.

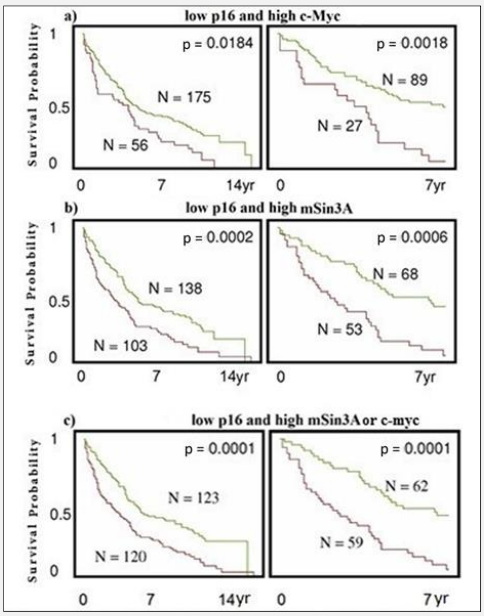

Figure 4. Survival analysis by Kaplan-Meier curves using manual scores for all patients (left) and stage I patients (right).

Wilcoxon test was considered significant if $p < 0.05$. Manual scores 0 and 1 were considered as low and scores 2 and 3 were considered as high expression. a) Survival difference for patients whose tumors had high c-Myc and low p16, b) high mSin3A and low p16, and c) low p16 with high c-Myc or high mSin3A.

tients ($p = 0.018$ and 0.001, respectively) and in Stage I patients ($p = 0.0018$ and 0.0006, respectively) (Figure 4). Furthermore, when the status of three proteins, p16, c-Myc, and mSin3A, was evaluated, low p16 with high c-Myc or high mSin3A was associated with reduced overall survival in all patients and in Stage I patients ($p = 0.0001$) (Figure 4).

DISCUSSION

Using NSCLC TMA we described here a novel screening system for evaluation of potential diagnostic and prognostic markers in cancer. We demonstrated that this semi-automated method can provide robust and reliable scoring for a large number of tissue cores present in a TMA. Beside eliminating the tedious task of manual scoring, CASA analysis provides the continuous high resolution scores that manual analysis does not. Thus the assessment on a continuous scale is superior to arbitrary scoring categories by a pathologist.

CASA, with a good resolution of scores, can calculate a biologically meaningful association of analysis that the manual scores cannot. Furthermore, it can help to identify markers that are associated to a particular patient population, histology type or particular cancer stage. Our stepwise analysis using the five clusters of 78 proteins showed that expression of some antigens were more closely associated to poor prognosis depending on gender, cancer stage, and cancer type. Our univariate analysis showed that expression of p16 and Her2 are marginally significant predictors for survival (Table 2). Further analysis using multiple proteins in the same molecular pathway suggests that p16 in combination with c-Myc or mSin3A is a strong predictor for survival (Figure 4).

Utilization of paired proteins in predicting prognosis has been recently documented [38,39]. Others have shown that the p16 protein decreases activity of c-Myc [40,41] and that binding of the p53 response element by c-Myc and mSin3A occurs in the MCF7 breast cancer cell line [42]. Our finding supports the suggestion that mSin3A may act closely with p16 and c-Myc in NSCLC. Our results suggest that the combinations of paired proteins could have significant association with patient outcome. This is supported by the complex nature of cancer development as a result of the activation of oncogenic signals and down regulation of tumor suppressor gene functions [43,44].

Strength and limitations

The major strength of the CASA method is its ability to perform a systematic and high throughput TMA analysis utilizing scanned images and facilitate complex statistical analysis. The normalization method for automated scoring here is less complicated and more reliable because of the exclusion of the minimum pixel range (scale 190 to 220) from the algorithm which represented stromal cell staining. Thus to remove stromal cells from reading, it is not necessary to stain double slides, one for the targeted protein and another for cytokeratin to normalize the scores [22-24]. In this study, we were able to confirm the reliability of CASA through Kaplan-Meier survival analysis using manual IHC scores of the same slide (Figure 4). However, independent validation will be needed to fully assess the findings from CASA since the current algorithm only measures the overall protein staining status disregarding subcellular localization and potential protein modification. In addition, intensity scores are also subject to errors when protein staining is less than highly specific to the tumor cells. Another limitation of CASA is that the digitalized scores cannot yet be easily applied to establish a clinically usable standard unit, and it is not yet possible to dichotomize CASA scores for the widely used Kaplan-Meier survival analysis. New statistical methods will have to be established to take full advantage of the continuous and highly informative digital scores for clinical usage. Finally, all IHC based evaluations are subject to the quality and specificity of the antibody, the nature of the antigen under investigation, and the morphology of the primary cancer being analyzed.

Acknowledgement:

We express our gratitude to the physicians who contributed to the primary tissue samples through the Armed Force Institute of Pathology (AFIP) and to AFIP for making updated follow-up and clinical information available for this study. We also thank members of LHC for critical discussions through the course of this study. This work was supported by the intramural research funds to the Center for Cancer Research at the National Cancer Institute. All authors participated in developing the content of this manuscript, preparing and reviewing the draft versions, and approving the final version.

Declaration of Interest:

There is no conflict of interest.

References:

1. Siegel R, Naishadham D, Jemal A. Cancer statistics, 2013. CA: A Cancer Journal for Clinicians 2013;63(1):11-30.

2. Toyooka S, Mitsudomi T, Soh J, et al. Molecular oncology of lung cancer. General Thoracic and Cardiovascular Surgery 2011; 59(8):527-37.

3. Howlader N, Noone A, Krapcho M, et al. SEER cancer statistics review, 1975-2009 (vintage 2009 populations). Bethesda, MD: National Cancer Institute 2012.

4. Carr LL, Finigan JH, Kern JA. Evaluation and Treatment of Patients with Non–Small Cell Lung Cancer. Medical Clinics of North America 2011;95(6):1041-54.

5. Howat WJ, Warford A, Mitchell JN, Clarke KF, Conquer JS, McCafferty J. Resin tissue microarrays: a universal format for immunohistochemistry. Journal of Histochemistry & Cytochemistry 2005;53(10):1189-97.

6. Bubendorf L, Kononen J, Barlund M, et al. Tissue microarray FISH and digital imaging: Towards automated analysis of thousands of tumors with thousands of probes. In: American Journal of Human Genetics: 1999: Univ Chicago Press, Chicago, IL 60637-1603 USA; 1999: A61-A61.

7. Tawfik O, Kimler B, Davis M, et al. Comparison of immunohistochemistry by automated cellular imaging system (ACIS) versus fluorescence in-situ hybridization in the evaluation of HER-2/neu expression in primary breast carcinoma. Histopathology 2006; 48(3):258-67.

8. Schoenberg Fejzo M, Slamon DJ. Frozen tumor tissue microarray technology for analysis of tumor RNA, DNA, and proteins. The American Journal of Pathology 2001;159(5):1645-50.

9. Dolled-Filhart MP, Gustavson MD. Tissue microarrays and quantitative tissue-based image analysis as a tool for oncology biomarker and diagnostic development. Expert Opinion on Medical Diagnostics 2012;6(6):569-83.

10. DeRisi J, Penland L, Brown PO, et al. Use of a cDNA microarray to analyse gene expression patterns in human cancer. Nature Genetics 1996;14(4):457-60.

11. Yoshida S, Arakawa F, Higuchi F, et al. Gene expression analysis of rheumatoid arthritis synovial lining regions by cDNA microarray combined with laser microdissection: up-regulation of inflammation-associated STAT1, IRF1, CXCL9, CXCL10, and CCL5. Scandinavian Journal of Rheumatology 2012;41(3):170-9.

12. Watanabe A, Cornelison R, Hostetter G. Tissue microarrays: applications in genomic research. Expert Rev Mol Diagn 2005; 5(2):171-81.

13. Aguilar-Mahecha A, Hassan S, Ferrario C, Basik M. Microarrays as validation strategies in clinical samples: tissue and protein microarrays. Omics: A Journal of Integrative Biology 2006;10(3): 311-26.

14. Abramovitz M, Leyland-Jones B. A systems approach to clinical oncology: focus on breast cancer. Proteome Science 2006;4(1):5.

15. Gillett C, Springall R, Barnes D, Hanby A. Multiple tissue core arrays in histopathology research: a validation study. The Journal of Pathology 2000;192(4):549-53.

16. Rabinovich A, Krajewski S, Krajewska M, et al. Framework for parsing, visualizing and scoring tissue microarray images. IEEE Trans Inf Technol Biomed 2006;10(2):209-19.

17. Chen W, Reiss M, Foran DJ. A prototype for unsupervised analysis of tissue microarrays for cancer research and diagnostics., IEEE Trans Inf Technol Biomed 2004;8(2):89-96.

18. Cardano M, Diaferia GR, Falavigna M, et al. Cell and tissue microarray technologies for protein and nucleic Acid expression profiling. Journal of Histochemistry & Cytochemistry 2013; 61(2):116-24.

19. Demichelis F, Magni P, Piergiorgi P, Rubin MA, Bellazzi R. A hierarchical Naïve Bayes Model for handling sample heterogeneity in classification problems: an application to tissue microarrays. BMC Bioinformatics 2006;7(1):514.

20. Malovini A, Barbarini N, Bellazzi R, De Michelis F. Hierarchical Naïve Bayes for genetic association studies. BMC Bioinformatics 2012;13(Suppl 14):S6.

21. Zu Y, Steinberg SM, Campo E, et al. Validation of tissue microarray immunohistochemistry staining and interpretation in diffuse large B-cell lymphoma. Leukemia & Lymphoma 2005;46(5):693-701.

22. Faith DA, Isaacs WB, Morgan JD, et al. Trefoil factor 3 overexpression in prostatic carcinoma: prognostic importance using tissue microarrays. The Prostate 2004;61(3):215-27.

23. Berger AJ, Camp RL, DiVito KA, Kluger HM, Halaban R, Rimm DL. Automated quantitative analysis of HDM2 expression in malignant melanoma shows association with early-stage disease and improved outcome. Cancer Research 2004;64(23):8767-72.

24. Giltnane J, Murren J, Rimm D, King B. AQUA and FISH analysis of HER-2/neu expression and amplification in a small cell lung carcinoma tissue microarray. Histopathology 2006;49(2): 161-9.

25. Fukuoka J, Fujii T, Shih JH, et al. Chromatin remodeling factors and BRM/BRG1 expression as prognostic indicators in non-small cell lung cancer. Clinical Cancer Research 2004;10(13):4314-24.

26. Fukuoka J, Dracheva T, Shih JH, et al. Desmoglein 3 as a prognostic factor in lung cancer. Human Pathology 2007;38(2):276-83.

27. Narlikar GJ, Fan H-Y, Kingston RE. Cooperation between complexes that regulate chromatin structure and transcription. Cell 2002;108(4):475-87.

28. Conway CM, O'Shea D, O'Brien S, et al. The development and validation of the Virtual Tissue Matrix, a software application that facilitates the review of tissue microarrays on line. BMC Bioinformatics 2006;7(1):256.

29. Sif S, Saurin AJ, Imbalzano AN, Kingston RE. Purification and characterization of mSin3A-containing Brg1 and hBrm chromatin remodeling complexes. Genes & Development 2001;15(5):603-18.

30. Zhang HS, Gavin M, Dahiya A, et al. Exit from G1 and S phase of the cell cycle is regulated by repressor complexes containing HDAC-Rb-hSWI/SNF and Rb-hSWI/SNF. Cell 2000;101(1):79-89.

31. Helms MW, Packeisen J, August C, et al. First evidence supporting a potential role for the BMP/SMAD pathway in the progression of oestrogen receptor-positive breast cancer. The Journal of Pathology 2005;206(3):366-76.

32. Mhashilkar AM, Stewart AL, Sieger K, et al. MDA-7 negatively regulates the β-catenin and PI3K signaling pathways in breast and lung tumor cells. Molecular Therapy 2003;8(2):207-19.

33. Tu Z, Zhuang X, Yao Y-G, Zhang R. BRG1 is required for formation of senescence-associated heterochromatin foci induced by oncogenic RAS or BRCA1 loss. Molecular and Cellular Biology 2013;33(9):1819-29.

34. Ota T, Maeda M, Suto S, Tatsuka M. LyGDI functions in cancer metastasis by anchoring Rho proteins to the cell membrane. Molecular Carcinogenesis 2004;39(4):206-20.

35. Zhang Y, Zhang B. D4-GDI, a Rho GTPase regulator, promotes breast cancer cell invasiveness. Cancer Research 2006;66(11): 5592-8.

36. Tsujimoto H, Hagiwara A, Sugihara H, Hattori T, Yamagishi H: Promoter Methylations of p16INK4a and p14ARF Genes in Early and Advanced Gastric Cancer. Correlations of the Modes of Their Occurrence with Histologic Type. Pathology-Research and Practice 2002;198(12):785-94.

37. Ma H-B, Hu H-T, Di Z-L, et al. Association of cyclin D1, p16 and retinoblastoma protein expressions with prognosis and metastasis of gallbladder carcinoma. World J Gastroenterol 2005;11(5): 744-7.

38. Warren L, Hughes A, Lai E, et al. Use of pairwise marker combination and recursive partitioning in a pharmacogenetic genome-wide scan. The Pharmacogenomics Journal 2007;7(3):180-9.

39. Ohta Y, Tanaka Y, Watanabe G, Minato H. Predicting recurrence following curative surgery in stage I non-small cell lung cancer patients using an angiogenesis-associated factor. J Exp Clin Cancer Res 2007;26(3):301-5.

40. Haas K, Staller P, Geisen C, Bartek J, Eilers M, Möröy T. Mutual requirement of CDK4 and Myc in malignant transformation: evidence for cyclin D1/CDK4 and p16INK4A as upstream regulators of Myc. Oncogene 1997;15(2):179-92.

41. Kan CE, Cipriano R, Jackson MW. c-MYC functions as a molecular switch to alter the response of human mammary epithelial cells to oncostatin M. Cancer Research 2011;71(22):6930-9.

42. Dannenberg J-H, David G, Zhong S, van der Torre J, Wong WH, DePinho RA. mSin3A corepressor regulates diverse transcriptional networks governing normal and neoplastic growth and survival. Genes & Development 2005;19(13):1581-95.

43. Vogelstein B, Kinzler KW. Cancer genes and the pathways they control. Nature Medicine 2004.10(8):789-99.

44. Gerstung M, Eriksson N, Lin J, Vogelstein B, Beerenwinkel N. The temporal order of genetic and pathway alterations in tumorigenesis. PLoS One 2011;6(11):e27136.

Supplementary Table 1. List of 78 antibodies used in CASA analysis.

	Name of antibody		Name of antibody		Name of antibody
1	AE1/AE3	27	Desmoglein-2	53	P16
2	Annexin	28	Desmoglein-3	54	p21
3	BAF155	29	Dsq1	55	p27
4	BAF170	30	Dsq2	56	p300
5	Bcatenin	31	E-Cadherin	57	P63
6	BRCA1	32	FAS	58	P-cadherin
7	Brg1	33	FOXM1	59	PCNA
8	Brm	34	GGH	60	PGP
9	Brq1	35	GSK3-B	61	PGP9.5
10	C20	36	HAT1	62	PTPN13
11	CC10	37	Hck	63	Rb
12	CD99	38	HDAC1	64	RbAP48
13	CDC20	39	HDAC2	65	Smad 2
14	CDK2	40	Her2	66	Smad 3
15	CEA	41	Hsnf2H	67	Smad 4
16	C-erbB3	42	Ini-1	68	Smad 6
17	c-Jun	43	JAB1	69	Smad 7
18	c-Myc	44	K903	70	Snf2H
19	CPE	45	LaminB	71	SNIP
20	Cyclin B1	46	LKB-1	72	Talin
21	Cyclin E	47	LY-GDI	73	TGFB
22	CyclinD1	48	Mad2	74	TGFBR1
23	Cytochrome C	49	Maspin	75	TGFBR2
24	DES1	50	mSin3A	76	Tip60
25	DES3	51	nm23	77	TTF1
26	Desmoglein-1	52	p14	78	XPC

Supplementary Table 2. Association of antibody staining status with clinical factors.

Gender	Female vs. Male	p16	< 0.05
	Male vs. Female	CDK2, DES1	
Age	> 60 years vs. < 60 years	LY-GDI	< 0.01
	< 60 years vs. > 60 years	TGFB-R1, C-erbB3, BRM	< 0.05
Stage	Stage I, II vs. Stage III, IV	P14, RB	< 0.01
Histology	Adenocarcinoma vs. Squamous cell carcinoma	TTF1, TGFB-R2, GSK3-B, Her2, CC10, CycB1, Smad-2, p27, Smad4, Smad7, p21, PTPN13, CEA, CPE, BRG1, Smad6, NM23, HCK, JAB1, FAS, p16	< 0.01
	Squamous cell carcinoma vs. Adenocarcinoma	K903, P63, HDAC2, P-cadherin, CD99, Annexin, DES3, DES1, Cytochrome-C	

Variable category highly expressed proteins p-value (*t*-test) *.
*** - Two-tailed *t*-test and assuming equal variance after log transformation of CASA scores, p < 0.01 is considered significant.**

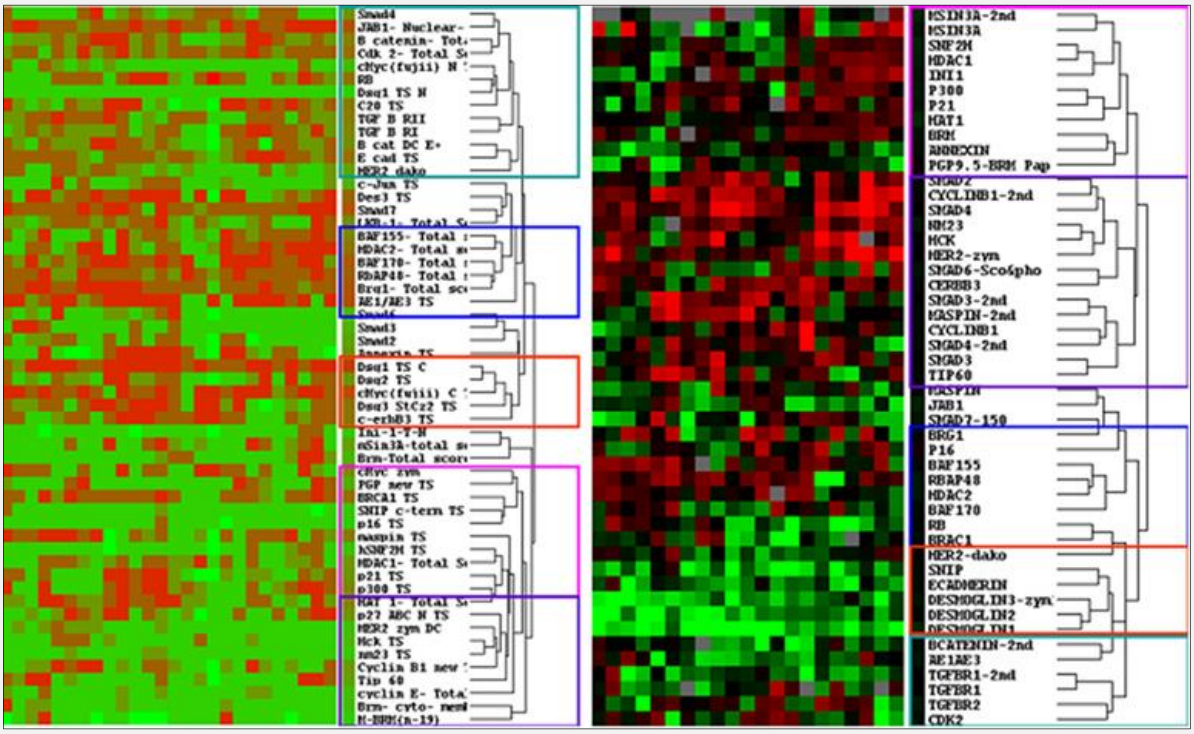

Supplementary Figure 1. The CASA scores subjected for all antibodies to hierarchical cluster analysis.

Hierarchical cluster of 55 manually scored proteins was nearly identical to the CASA scored protein. Left panel is hierarchical cluster of manual scores and right panel is hierarchical cluster of CASA scores. Similarity of each paired sub-cluster is shown with the same color in each panel.